Reduction of speckles in retinal reflection

Vassilios Albanis,[a] Erez N. Ribak, and Yuval Carmon[b]
Department of Physics, Technion - Israel Institute of Technology, Haifa 32000, Israel

(Received 30 April 2007; accepted 28 June 2007)

Speckle noise can deteriorate the quality of wave-front sensors measuring ocular aberrations. To counter that, a narrow laser beam was acoustically modulated before entering the eye and creating a spot on the retina. Light was scattered back through the aberrations into the sensor. The increased spot size, wider angular spread, and temporal modulation of the incoming beam averaged out the speckles, producing a more uniform response of the wave-front sensor. The method applies also to retinal imagers and to nonbiological speckle. © *2007 American Institute of Physics*.
[DOI: 10.1063/1.2761835]

Wave-front sensing is used to examine the aberrations of optical systems, and in adaptive optics, to provide feedback for real-time correction. In many applications, where there is no light source available as a reference behind the examined system, a narrow beam passes through the system to create a small beacon. Light is scattered back from the beacon through the aberrations to be measured by a wave-front sensor. Wave-front sensing has spread from optics and astronomy into other fields such as ocular optics. In the case of ocular wave-front sensing, a strong speckle field forms due to the random interference of the coherent light with the highly anisotropic tissues comprising the retina. The resulting nonlinear response and saturation of the sensor reduce the accuracy of the reconstructed wave front.[1] A number of different methods have been devised in an effort to reduce the speckle effect, such as smoothing in software, scanning and descanning mirrors,[1,2] or diffusers such as rotating scatter plates, multimode or dispersive fibres.[3] Speckle reduction can also be achieved by decreasing the coherence of the light, namely, by using superluminescent diodes[3] (SLDs), femtosecond lasers, and even white light. However, low coherence and directionality are usually opposing requirements: the light efficiencies of SLDs, white light source, and fiber-coupled beams are low and require more lenses and pinholes for collimation. For other purposes altogether, speckle was reduced by acoustic interaction with the light beam,[4,5] or directly with a biological tissue,[6] which is not practical for imaging of the human eye.

We present a simple method to reduce the speckle noise during measurements of aberrations. We average the speckle field by widening the beam slightly on the cornea, in real space, in k space, and in time. This in turn scatters off a larger volume in the retina, and off a wider range of angles, which is important because of retinal anisotropy. Thus, the random speckle effect is averaged out to a significant degree. Instead of using lenses or mechanical scanners to widen the beam, we achieved it by diffracting a laser beam inside an acousto-optic cell. The device has been used previously to produce a Hartmann-Shack (HS) sensor with a variable pitch, where the lenslet array is replaced by caustics formed by two standing acoustic waves, perpendicular to each other and to the incoming laser beam.[7] Here we operate in the far field, in the Raman-Nath regime, and the wider light spot is partially modulated, in space and time, by fringes from the higher orders of diffraction.

We implemented our method with a minimal modification of the HS wave-front sensing arrangement (Fig. 1). A polarized laser diode, operating at 780 nm, illuminated the subject eye, with a nominal beam diameter on the cornea of $\lesssim$1 mm. The acoustic cell was inserted immediately after the laser diode. A beam splitter reflected 8% of the light into the eye, some 40 cm down the beam from the cell. The laser power was tuned by an analyzer to 20–30 μW on the retina. We made no effort to depolarize the beam, to keep the system simple at the cost of slightly worse speckle. The unwanted off-axis corneal reflection was removed by an aperture or an analyzer. The light was scattered back through the pupil and imaged onto a glass lenslet array, with up to half a dozen lenslets per millimeter on the cornea. The multiple foci were relayed again to an uncooled, standard video camera. In an additional optical arm of the setup, a second camera was trained on the subject's retina to acquire the instantaneous point spread function. When observed in real time by the subjects' other eye, they reported an extreme similarity between the subjective and objective impressions.

For validation we used an artificial eye, where the retina, at the focus of a misaligned lens, was simulated by a moving white paper. The speckle statistics were different from a live

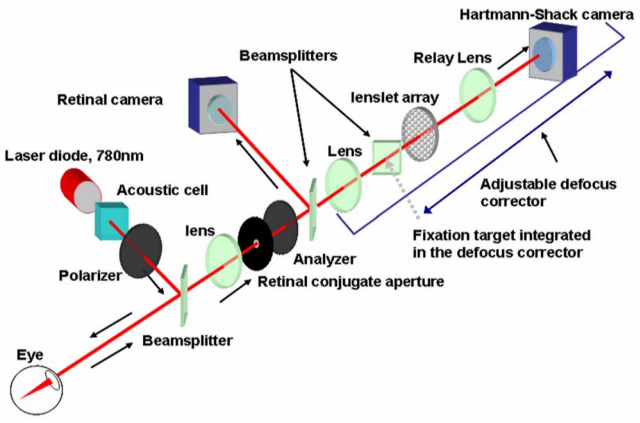

FIG. 1. (Color online) Ocular wave-front sensor. The acoustic cell is positioned immediately after the laser diode. After scattering from the retina, the beam is relayed to the HS lenslet array and again to the HS camera. The beam is recorded by the retinal camera.

[a]Electronic mail: valbanis@physics.technion.ac.il
[b]Also at Shamir Optical Industry, Kibbutz Shamir, Upper Galilee 12135, Israel.

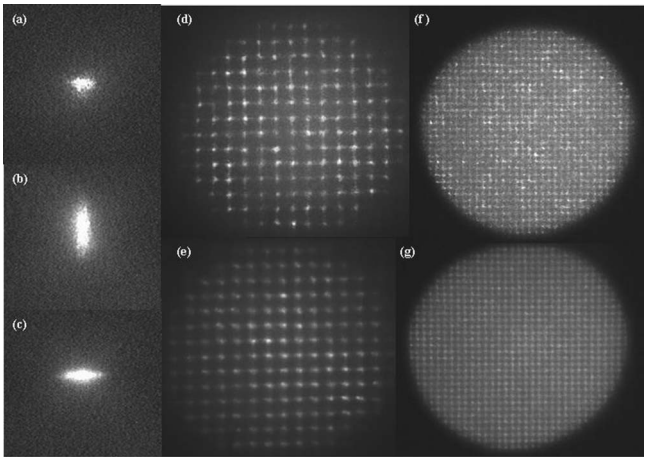

FIG. 2. Retinal and HS images (see also supplementing movies): (a) retinal spot, cell off; (b) retinal image, cell on, y diffraction; (c) retinal image, x diffraction; (d) pupil image, cell off, with speckle and saturation; (e) same HS pattern, cell on, with reduced speckle; (f) pupil image, dense lenslets, cell off; and (g) same, cell on.

eye,[1] but strong enough to saturate the detector and distort the HS pattern. With the cell on, saturation disappeared. We used a Fourier method[8] to convert each HS grid of spots into wave-front slopes, and then to the wave-front itself.[9] With this analysis it is advantageous to use denser sampling, so we used smaller lenslets. While the ~ 80 μm retinal spot is not resolved by these lenslets, significant smoothing is visible even when using larger lenslets (Fig. 2). We compared one wave front calculated from an average image from 100 HS speckled images to the average of another 100 calculated wave fronts, with the cell resonating at 1.25 and at 3.30 MHz. All results were equal to within a few percent.

Next, we examined the aberrations of three experienced subjects, ages 32 to 56, with +1.5 to −4.5 D defocus, and −0.25 to −1.0 D cylinder. The subjects were asked to fix their gaze on a target placed at infinity on or within 2° of the fovea. The pupils were dark adapted, with diameters between 4 and 7 mm. The images of the HS patterns with the cell off and on were acquired consecutively with minimal eye changes. We captured a series of 12 HS images within 4 s. Below 1.5 MHz, the laser spot appeared diffractively elongated, but at the higher frequencies the orders were distinct. The supplemental retinal movie[10] shows how, by tuning the frequency, elongation occurred in x and/or in y according to the cell mechanical resonance direction. The size of the beam on the cornea was 1–2 mm depending on the acoustic power. If the eye was focused at infinity and the cell was 40 cm away, the spot was extended by ~ 40 μm on the retina, resolving the first and higher orders. Reduction of the speckle noise was achieved in all subjects.

A simple model can describe the method. The incoming light produces frequency-modulated multiple beacons with reflected amplitude

$$S(x,t) = D(x)\{V_0 + V_1 \exp[i(K_1 x + \Omega t)] + \cdots\}\Psi(x)L(x), \tag{1}$$

where $D(x)$ is the laser spot spread, and $V_k(k=0,1,\ldots)$ is the amplitude of the kth diffraction order, with K_k and Ω its spatial and temporal modulation frequencies. The relative powers of the orders can be varied,[11] so that $V_0=0$. $\Psi(x)$ is the reflection off the retina, and $L(x)$ is the back-propagated HS lenslet aperture (usually an Airy pattern). We model the retinal scattering function in Eq. (1) as

$$\Psi(x) = [R + \amalg_C(x)]\exp[i\varphi(x)]. \tag{2}$$

Backscatter of blood vessels or ganglion cells is represented by a rather flat response R, while the highly anisotropic return from the photocells is given by a comb function $\amalg_C(x)$ of spacing C (in a full two-dimensional model, the cells are organized on a near-hexagonal grid[12]). The random phase φ varies on a scale finer than C, where $C < K_1^{-1}$,

$$\langle \varphi(x)\varphi(x+C)\rangle \ll 1, \tag{3}$$

making the reflected phase from each photocell independent of its neighbors. When the sensor erroneously images the volume above or below the retina, this assumption of short-term correlation breaks down and the speckles drop in size.[1] We assume that the retina does not move during the fast exposures, and changes are ignored which might be due to movement of the eye or to heartbeat. In Eq. (1), we did not include the separation of the acousto-optic orders nor their angular diversity, although they further contribute to averaging of the speckles. Thus, the main effect is the addition of the random phase terms in Eq. (2) to the acoustic time-variable phase in Eq. (1), creating a fast-varying speckle. The image in each lenslet focus, conjugate to the beacon, is the average power of Eq. (1), namely, $\langle |S(x,t)|^2\rangle$. As a result of averaging of the boiling speckle over space and time, we obtained a significant reduction of saturation and subsequent uniformity of the HS pattern.[13] Figure 2 and the second movie[10] shows how the lenslet foci, single and groups, which were strongly scintillating, now had nearly equal and smooth intensity distribution.

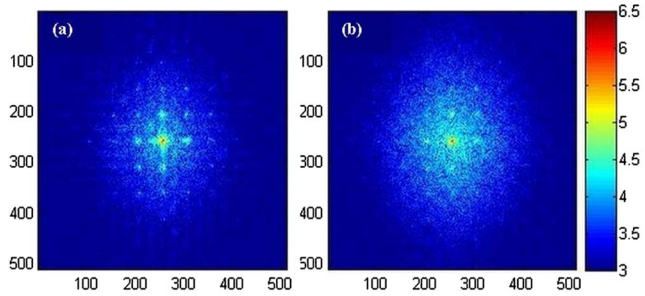

FIG. 3. (Color online) Power spectrum of a HS pattern with (a) cell on and (b) off (log scale). While the signal is fully conserved, the background noise drops when the cell is on.

Figure 3 shows the Fourier transform of one of the HS patterns. While the signal components in Fourier space were essentially identical, the background noise dropped appreciably when the cell was running. The overall standard deviation among the 12 frames, each $768\times568\times8$ bit pixels in size, was 7.70×10^{-4}, dropping off with application of the acoustic cell to 4.14×10^{-4}. Thus, the available light is used more efficiently, as less of the signal is lost due to scattering into higher frequencies and to camera saturation. The reco-

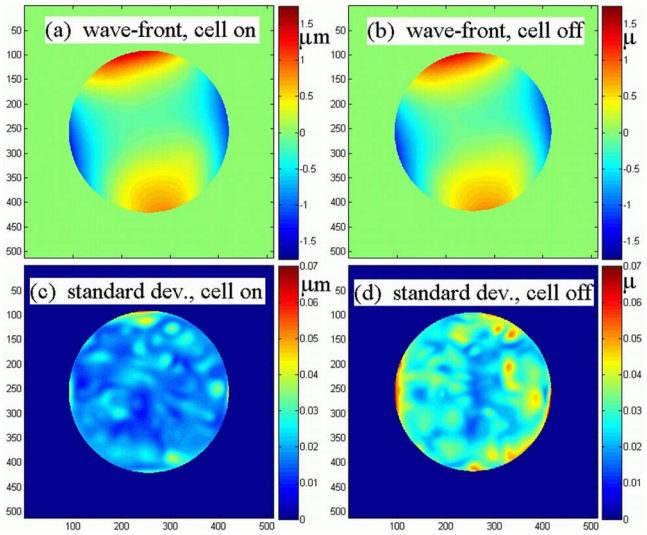

FIG. 4. (Color online) Average of 12 wave fronts with cell on (a) and off (b); (c) and (d) associated standard deviations. Accommodation and pupil size changed slightly between acquired sets. Piston, tip, tilt, and defocus were subtracted from the wave front.

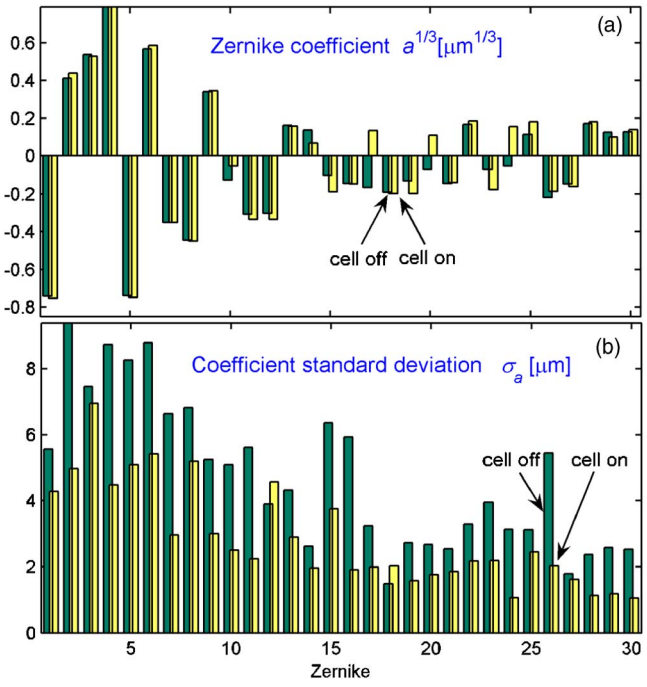

FIG. 5. (Color online) Zernike coefficients of Fig. 4 (top) and their distributions (bottom). The live eye contributed to some of the difference between the cell being off (green bars) and on (yellow bars). To bring out the higher terms, we show the cubic root of the Zernike coefficients.

structed wave fronts of a 7 mm pupil are shown Fig. 4. The despeckled wave front is less noisy while retaining the same features as the speckled one. Similar results are visible in the Zernike decomposition of the wave front (Fig. 5).

In summary, the method we show results in reduction of variability of the measurements, more uniform images, better use of the dynamic range of the detector, and simplicity of setup. While the light source can still be a collimated superluminescent diode or white light, we show that a simpler laser can also be used, being easier to align and point and more power efficient. Most of the effect results from acoustic modulation of the phase of the returned speckle and its averaging. Other wave-front sensors such as the pyramid[14] or curvature,[15] or image sharpening in adaptive optics,[16] also requiring speckle-free reference sources, can gain from this solution. Finally, the application is valid for other speckle-limited sensing, such as scanning-laser ophthalmoscopy, optical coherence tomography, tissue microscopy, laser beacons, and nonbiological imaging.

Partial support was available by the French-Israeli Science Fund. Engineering assistance from Shamir Optical Industry is greatly appreciated.

[1] A. V. Larichev, P. V. Ivanov, I. G. Iroshnivkov, and V. I. Shmal'gauzen, Quantum Electron. **31**, 1108 (2001).
[2] H. Hofer, P. Artal, B. Singer, J. L. Aragon, and D. R. Williams, J. Opt. Soc. Am. A **18**, 597 (2001).
[3] J. Rha, R. S. Jonnal, K. E. Thorn, J. Qu, Y. Zhang, and D. T. Miller, Opt. Express **14**, 4552 (2006).
[4] J. Selb, S. Leveque-Fort, L. Pottier, and A. C. Boccara, C. R. Acad. Sci., Ser IV: Phys., Astrophys. **2**, 1213 (2001).
[5] L. Wang, T. Tschudi, M. Boeddinghaus, A. Elbert, T. Halddorsson, and P. Petrusson, Opt. Eng. **39**, 1659 (2000).
[6] D. P. Popescu, M. D. Hewko, and M. G. Sowa, Opt. Commun. **269**, 247 (2001).
[7] E. N. Ribak, Opt. Lett. **26**, 1834 (2001).
[8] Y. Carmon and E. N. Ribak, Appl. Phys. Lett. **84**, 4656 (2004).
[9] C. Canovas and E. N. Ribak, Appl. Opt. **46**, 1830 (2007).
[10] See EPAPS Document No. E-APPLAB-91-109729 for movies showing the diffracted spot on the retina and the speckle reduction in the Hartmann Shack. This document can be reached via a direct link in the online articles HTML reference section or via the EPAPS homepage (http://www.aip.org/pubservs/epaps.html).
[11] W. R. Klein and B. D. Cook, IEEE Trans. Sonics Ultrason. **SU-14**, 123 (1967).
[12] S. Marcos, S. A. Burns, and J. C. He, J. Opt. Soc. Am. A **15**, 2012 (1998).
[13] B. Vohnsen, I. Iglesias, and P. Artal, J. Opt. Soc. Am. A **22**, 2318 (2005).
[14] I. Iglesias, R. Ragazzoni, Y. Julien, and P. Artal, Opt. Express **10**, 419 (2002).
[15] S. Gruppetta, L. Koechlin, F. Lacombe, and P. Puget, Opt. Lett. **30**, 2757 (2005).
[16] S. Zommer, E. N. Ribak, S. G. Lipson, and J. Adler, Opt. Lett. **31**, 939 (2006).